

# Thin-layer detection from the cone resistance rate of change

H.B. Hammer

*Dr.techn. Olav Olsen AS, Trondheim, Norway*

S. Nordal

*Norwegian University of Science and Technology (NTNU), Norway*

J.-S. L'Heureux & H. Skrede

*Norwegian Geotechnical Institute (NGI), Norway*

**ABSTRACT:** True determination of soil parameters for thin clay layers in sand or silts from CPTU measurements is challenging. Cone resistance in thin layers is influenced by the surrounding layers resulting in unrepresentative measurements. Measurements should be corrected for this effect prior to interpretation of parameters. Such correction requires accurate information about the thickness of the thin layer. Previous studies have shown that the pore pressure parameter of the CPTU may not properly identify the layer interfaces for thin clay layers in sand. In this study a “cone resistance rate of change” parameter is suggested for thin-layer interface detection. Results from recently performed physical experiments at NTNU as well as from prior studies are used to evaluate the ability of this parameter to detect thin layers of clay in sand. The parameter appears to detect layer interfaces with good accuracy, even for layers with thickness as thin as the cone diameter. The results suggest that the approach may estimate layer thickness quite well and aid towards efficient correction of cone resistance to achieve more realistic soil parameters for thin clay layers in sand.

## 1 INTRODUCTION

The near-continuous measurements of CPTU parameters cone resistance ( $q_c$ ,  $q_t$ ), pore pressure ( $u_2$ ) and skin friction ( $f_s$ ) provide great details of the subsurface. The combined response of these parameters can be used for characterization of materials for thick homogenous sediments. Close to layer interfaces and in thin layers the measurements may be significantly influenced by multiple materials simultaneously. Accurate characterization and interpretation of geotechnical parameters of thin layers requires correction of these effects, which in turn depends on the layer thicknesses. It is therefore important to obtain detailed information of the layer interfaces. The  $u_2$  parameter may not provide accurate measurement of the thickness of such thin clay layers (Hird et al. 2003, van der Linden et al. 2018, Hammer et al. *in press*).

This study assesses the possibility of detecting layer interfaces from cone resistance measurements based on its rate of change. Layering between different combinations of sand and clay layers are assessed from physical experiments. There are complex relations between the mechanical properties of different materials and the measured cone resistance. However, the

evaluations in the current study relies exclusively on the cone resistance measurements and soil type (i.e., sand or clay), rather than the geotechnical parameters of the soils.

## 2 TRANSITION AND THIN-LAYER EFFECTS

Values of the cone resistance that only reflect a single, homogenous material is labeled the *characteristic* cone resistance of the material. Close to a layer interface between different materials, the measured cone resistance may deviate from the characteristic cone resistance. This is due to factors such as the cone geometry and difference in stiffness and strength between the materials. The distances of transition effects in the materials are labeled sensing- and developing distance, as illustrated in Figure 1 (a).

In a thin layer, where the layer thickness is less than the sum of the sensing- and developing distance of the thin layer, the extreme value will not equal the characteristic cone resistance, known as *thin-layer effects*. An example of this is illustrated in Figure 1 (b). The characteristic cone resistance in thin layers can be estimated through correction factor,  $K_H$  (Youd & Idriss 2001):

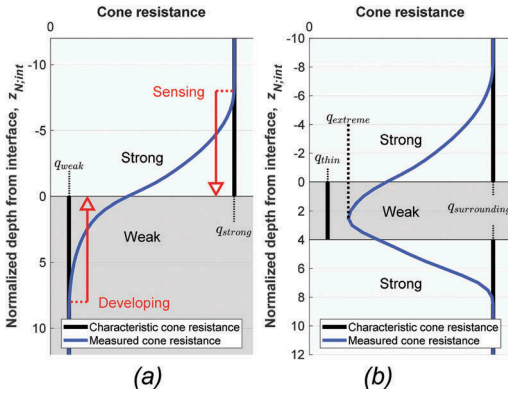


Figure 1. Illustration of transition- and thin-layer effects for (a) a two-layered composition and (b) a three-layered composition.

$$q_{thin} = K_H \cdot q_{extreme} \quad (1)$$

Values of  $K_H$  is less than or equal 1 in thin weak layers, e.g., Figure 1(b). For the opposite case, in thin strong layers, values are greater or equal 1. Factors of  $K_H$  are proposed for thin sand layers in clay (i.e., thin strong layers) based on field data and experiments. It is however a lack of proposed correction factors for thin weak layers.

The proposed correction factors are typically dependent on the thin layer thickness compared to the cone diameter ( $H/d_c$ ) and the contrast between the characteristic cone resistance of the thin layer and the surrounding layers (i.e.,  $q_{thin}/q_{surrounding}$ ). More advanced methods of thin layer corrections have been proposed, most noticeably the inverse filtering procedure (Boulangier & DeJong 2018).

### 3 CONE RESISTANCE RATE OF CHANGE

The cone resistance is in this study presented against the depth of the cone tip ( $z$ ) normalized on the cone diameter ( $d_c$ ):

$$z_N = \frac{z}{d_c} \quad (2)$$

The depth is furthermore referenced to the depth of a layer interface ( $z_{int}$ ):

$$z_{N:int} = \frac{z - z_{int}}{d_c} \quad (3)$$

The subscript of the cone resistance measurement type is omitted in this study. I.e., the symbol  $q$  is used rather than  $q_c$  or  $q_t$ . The latter is the corrected cone resistance for pore pressure due to unequal area effects. Each measurement of  $q$  can be labeled with and index

$i$ , i.e.,  $q_i$ . These values have a corresponding measurement depth  $z_i$ , where values of depth are increasing with increasing indices.

Assuming a constant characteristic cone resistance for each layer, such as for the examples in Figure 1, the derivate of the measured cone resistance is expected to reflect the transition effects. The derivate can be expressed as the change of measured cone resistance over the distance between measurements. The derivate of  $q$  becomes:

$$\left( \frac{\Delta q}{\Delta z_N} \right)_i = \frac{q_{i+1} - q_i}{z_{i+1} - z_i} \cdot d_c \quad (4)$$

The unit of this parameter is given in units of stress, e.g., MPa.

Hammer et al. (in press) proposed a normalized parameter of cone resistance rate of change,  $q'_i$ , defined as  $\Delta q/\Delta z_N$  divided by the average cone resistance between the two depths:

$$\begin{aligned} q'_i &= \left( \frac{\Delta q}{\Delta z_N} \right)_i \cdot \frac{1}{0.5 \cdot (q_{i+1} + q_i)} \\ &= \frac{q_{i+1} - q_i}{z_{i+1} - z_i} \cdot \frac{2 \cdot d_c}{q_{i+1} + q_i} \end{aligned} \quad (5)$$

An advantage of normalizing the derivative of the average measurement is an increased emphasize on transition effects in weak materials. This parameter showed promise for detecting interfaces for thin clay layers.

The procedure of Boulangier & DeJong (2018) consisted of three main components, where the first two corrects measurements of cone resistance for thin layer effects. The last component attempts to correct for transition effects. Profiles corrected for thin-layer effects are evaluated based on the rate of change to identify and approximate sharp transition (i.e., interfaces). The resistance rate of change was defined as:

$$m_i = \ln \left( \frac{q_{i+1}}{q_i} \right) \cdot \frac{d_c}{z_{i+1} - z_i} \quad (6)$$

Interfaces was in the study determined primarily based on whether the values of  $m$  (calculated from cone resistance profiles corrected for thin-layer effects) were greater than 0.1.

Both  $q'$  and  $m$  are parameters describing the relative change in cone resistance over normalized distances ( $\Delta z_N$ ). The two parameters are compared for various relations of  $q_{i+1}/q_i$  over one cone diameter distance ( $\Delta z_N = 1$ ) in Figure 2. The parameter  $m$  is for this situation represented with  $f_1$  while  $f_2$  represents  $q'$ . Two additional relationships are added for comparison,  $f_3$  and  $f_4$ , these represent  $\Delta q/\Delta z_N$  normalized on  $q_i$  and  $q_{i+1}$  respectively. From this it is evident that there is

a negligible difference between  $q'$  and  $m$  for small relative changes,  $q_{i+1}/q_i$ . Due to the numerical advantages of computing the function  $f_1$  rather than  $f_2$ , the parameter  $m$  is used in this study for the cone resistance rate of change. Each measurement of  $m_i$  is assigned to the average depth between  $z_i$  and  $z_{i+1}$ . Note that if the distances between measurements are approximately constant, this only results in a change the reference depth.

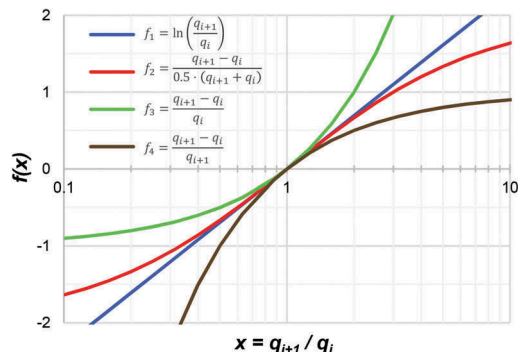


Figure 2. Different measurements of cone resistance rate of change.

The advantages of the cone resistance rate of change  $m$  compared to the derivative  $\Delta q/\Delta z_N$  is highlighted through an example of one of the physical experiments from de Lange (2018). Figure 3 presents values of  $q$  together with calculated values of  $m$  and  $\Delta q/\Delta z_N$ . The soil sample has thin alternating clay and sand layers of  $H=3.2d_c$  between two sand layers. Three measurements of the same sample were performed with the sample exposed to a surcharge load of 25, 50 and 200 kPa.

The two primary advantages of  $m$  compared to  $\Delta q/\Delta z_N$  are firstly the apparent independency on the stress level, as observed from the figure. Secondly, values of  $m$  appear to reach extreme values at constant distances to the layer interfaces. The second advantage will be explored in chapter 5.

## 4 DATA FROM PHYSICAL EXPERIMENTS

### 4.1 Experiments

The normalized cone resistance rate of change was applied to measurements from physical experiments on layered sand and clay. The aim to determine its ability to detect layer interfaces as well as characterize thin-layer- and transition effects. Results of recent experiments performed at NTNU are evaluated together with multiple studies from literature. A list of all references of the experiments evaluated in this study is presented in Table 1.

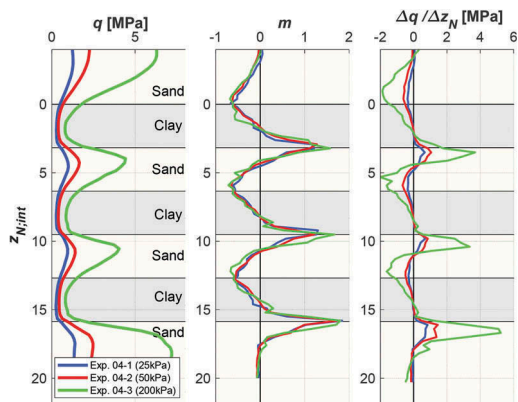


Figure 3. Example of values of  $m$  compared to  $\Delta q/\Delta z_N$ . Measurements from de Lange (2018), containing multiple thin clay and sand layers of thicknesses of  $H=3.2d_c$  between sand layers. The names of the series indicate the applied surcharge.

The physical experiments are performed on constructed samples of layered sands and clays in chambers. Preparation methods and material properties of sands and clays vary between the different experiments. In general, the sands in the created samples are described as clean, uniform, and homogenous. Clay layers are also homogenous and primarily described as soft. The relations between the material properties and the measured cone resistance are not evaluated in this study.

The CPT probes used in all experiments have  $60^\circ$  apex while the cone diameters are varying from 1 to 3.6 cm. The diameter size (rounded in millimeters) of the different experiments are shown in Table 1.

The results of Hammer (2020) and Skrede (2021) are corrected for unequal area effects, however, the differences in thin clay layers were found to be neglectable. The measurements from literature are primarily not corrected for unequal area effect.

Table 1. Physical experiments of cone penetration in calibration chambers of layered sands and clays evaluated in this study.

Reference	Materials	$d_c$ [cm]
van der Berg (1994)	Sand, clay	3.6
Teh et al. (2010)	Sand, clay	1
Mlynarek et al. (2012)	Sand, clay	3.6*
Tehrani et al. (2017)	Sand	3.2
van der Linden et al. (2018)	Sand, clay	2.5
de Lange (2018)	Sand, clay	2.5
Wang (2019)	Clay	1
Hammer (2020)	Sand, clay	3.6
Skrede (2021)	Sand, clay	3.6

\* Probe properties were not found, a standard size ( $10\text{cm}^2$ ) is assumed

## 4.2 Results from chamber tests at NTNU

The problem of thin clay layers in sand has been studied through large scale physical experiments in a CPTU chamber at NTNU (Norwegian University of Science and Technology) in Trondheim during the last two years. Samples were constructed in a chamber of 1.2 m diameter and 1 to 2.2 m height. Multiple cases of varying thin-layer thickness were tested at varied stress states. Details on the experiments and results are presented in the MSc theses Hammer (2020) and Skrede (2021). A combined six sample cases were constructed and tested in the two studies, named E1 - E6.

## 4.3 Results from literature

Multiple studies have been performed on physical experiments of cone penetration in layered sand and/or clays. The experiments that are found to be relevant for this study are summarized in Table 1. The cone resistance measurements of these studies were digitized from figures in a detailed manner. Depth measurements were converted to the normalized depth of the cone tip below a layer interface ( $z_{N;int}$ ). The measurements from literature were interpolated at  $0.3d_c$  intervals since the actual intervals between measurements are unknown. For a standard cone with area  $10 \text{ cm}^2$  this corresponds to measurements each 1 cm.

# 5 RESULTS

## 5.1 Sand

The profiles of two experiments with dense over loose sand from Tehrani et al. (2017) are presented in Figure 4 (top). Minimum values of  $m$  coincide with the layer interface with values of -0.2 and -0.3. The study defined sensing lengths of  $5.1d_c$  for both experiments, reflecting approximately the distance from where  $m$  changes sign to the layer interface. Developing distances were defined as  $2.2d_c$  and  $2.4d_c$ , respectively.

Figure 4 (bottom) show the opposite layering, i.e., loose sand over dense sand. The maximum values of  $m$  for the two experiments were 0.5, these values occur at a distance  $1-2d_c$  prior to the layer boundary. Sensing distances were described as  $2.8 d_c$  and  $3 d_c$ , respectively, while developing distances were  $3.8 d_c$  and  $3.9 d_c$ .

## 5.2 Clay

Transition effects between clay layers was evaluated in the study of Wang (2019). Results of experiments with stiff clay over soft clay are presented in the top of Figure 5. Values of  $m$  decrease only from a distance of about  $1d_c$  prior to the layer interface. The transition towards the characteristic cone resistance of the soft clay layer (i.e., the developing length) appear to be over about  $4-6d_c$ .

Results of experiments with soft over stiff clay are shown in Figure 5 (bottom). Sensing distance is for this layering case about  $1d_c$  as well, while the developing distance appear to be about  $2d_c$ .

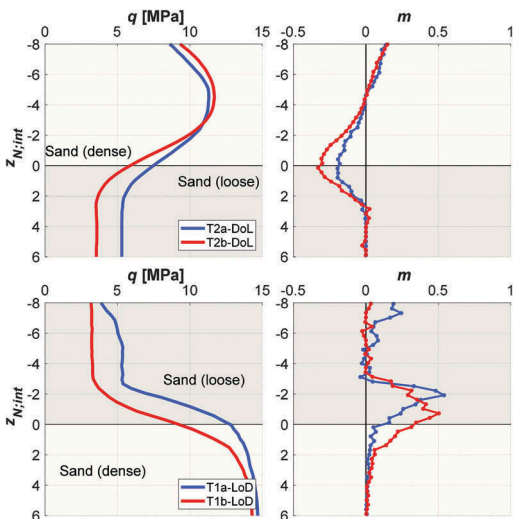


Figure 4.  $q$  and  $m$  profiles for layered sand, experiments of Tehrani et al. (2017). Top: dense over loose sand. Bottom: Loose over dense sand.

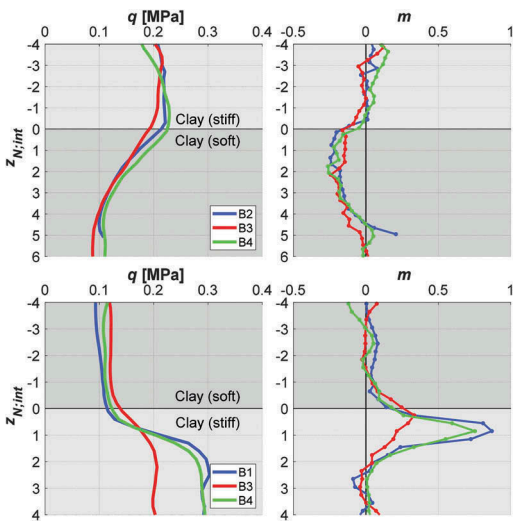


Figure 5.  $q$  and  $m$  profiles for layered clay, experiments from Wang (2019). Top: stiff over soft clay. Bottom: soft over stiff clay.

## 5.3 Sand and clay

Various studies have included experiments on thick layers of sand and clay. These include van der Berg (1994), Teh et al. (2010), Mhynarek et al. (2012), van der Linden et al. (2018) and Skrede (2021). Four of these are presented in Figure 6 for a thick sand layer over clay. Three of the  $q$ -profiles are increasing until  $2-3d_c$  distance to the interface due to the proximity to the top surface of the sample. This causes greater uncertainty in the interpretation of sensing distance. An approximation of the sensing distance may be  $2-3d_c$  for these three

measurements and  $5-6d_c$  for Mlynarek et al. (2012). Extreme values of the  $m$ -profiles were between  $-0.8$  and  $-0.6$ , reached within  $1d_c$  of the actual layer boundary.

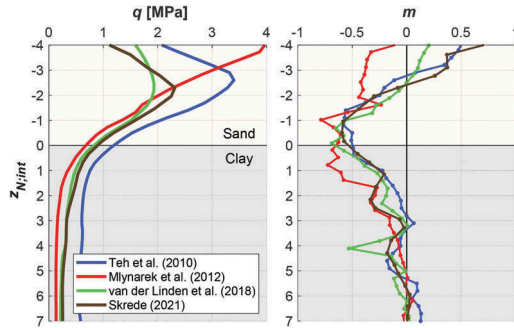


Figure 6.  $q$  and  $m$  profiles for two-layered samples of sand over clay from multiple studies.

The opposite layering is presented in Figure 7. Similar to the two-layered clay in section 5.2, the clay layers exhibit a very short sensing distance of about  $1d_c$ . The contrast (i.e., ratio) between the characteristic cone resistance of the bottom sand layer and the clay layer varies from 25 to 100. The developing distance displayed in the sand layer appear to be approximately  $3d_c$ . Extreme values of the  $m$ -profiles vary from 2.6 to 4.4 and occur at the layer interface.

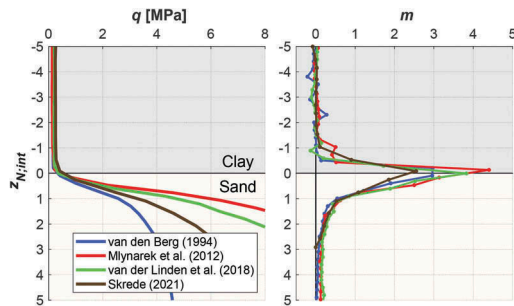


Figure 7.  $q$  and  $m$  profiles for two-layered sand and clay from multiple studies. Top: sand over clay. Bottom: clay over sand.

#### 5.4 Thin clay layer in sand

Measurements from NTNU experiments E2 (Hammer 2020) and E5 (Skrede 2021) of thin clay layers with thickness  $0.56-2.2d_c$  are presented in Figure 8. The characteristic cone resistance of the sand layers were about 10 times that of the clay layer. The  $m$ -profiles for the three different layer thicknesses primarily have extreme values for the top transition of between  $-0.6$  and  $-0.5$ . These occur very close to the clay layer interface. Extreme values of  $m$  for the bottom transition occur  $0-1d_c$  below the bottom interface. The extreme values decrease with

decreasing layer thickness. Sensing and developing distances in the sand can be approximated to  $2-3d_c$  and  $2d_c$ , respectively.

#### 5.5 Multiple thin sand and clay layers

Numerous experiments on samples with multiple thin sand and clay layers of equal thickness is presented in the study of de Lange (2018). Here, three of these are presented. The first is the “exploratory test 4” presented in Figure 3 with thicknesses  $3.2d_c$ . Figure 9 and Figure 10 present respectively “soil model 02” with layer thicknesses  $1.6d_c$  and “soil model 08” with layer thicknesses  $0.8d_c$ . Both the experiment with thicknesses  $3.2d_c$  and  $1.6d_c$  reaches extreme values of  $m$  very close to or at the interfaces. Extreme values of  $m$  prior to clay layers and sand layers are respectively about  $-0.6$  and  $1-1.8$ . For the sample with layer thicknesses  $0.8d_c$  the values of  $m$  are significantly lower than the other two experiments. However, the shape of the  $m$ -profile is largely the same and extreme values of  $m$  correspond to interfaces fairly well.

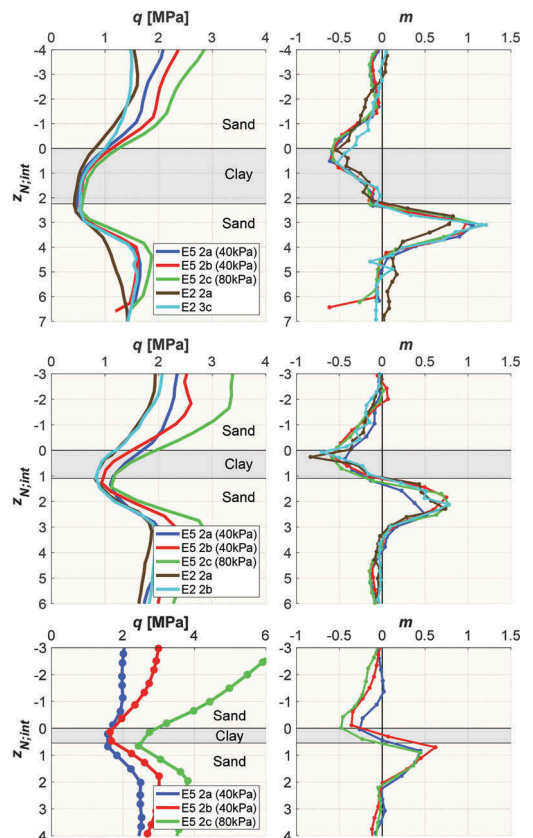


Figure 8.  $q$  and  $m$  profiles for thin clay layers in sand. Experiments from Hammer (2020) and Skrede (2021). Top:  $H = H=2.2d_c$ . Middle:  $H=1.1d_c$ . Bottom:  $H=0.56d_c$  (each measurement point is marked with dots).

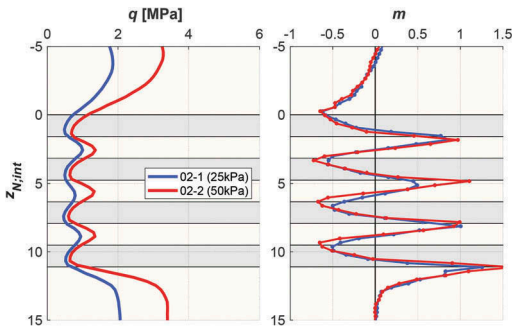


Figure 9.  $q$  and  $m$  profiles for multiple thin layers of sand and clay,  $H=1.6d_c$ . Experiments from de Lange (2018).

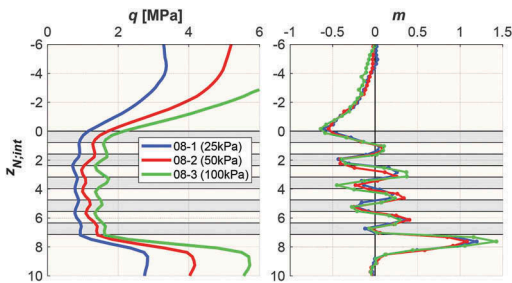


Figure 10.  $q$  and  $m$  profiles for multiple thin layers of sand and clay,  $H=0.8d_c$ . Experiments from de Lange (2018).

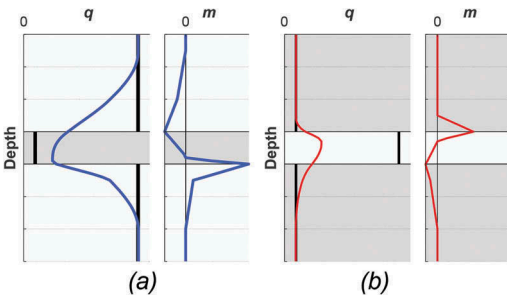


Figure 11. Illustration of the expected thin-layer effects in (a) a thin clay layer embedded in sand and (b) a thin sand layer embedded in clay. Black lines are the characteristic cone resistance.

## 6 DISCUSSION

### 6.1 Sensing and developing lengths

It is evident from the experiments that the sensing and developing distances of sand and clay are significantly different. While penetration in sands exhibit an almost equal sensing- and developing distances, there are large differences in clays. In clays, the sensing distance appear to typically be about one cone diameter in front of the cone tip, while the developing distance are up to six times the amount. This difference is considered to be

key in understanding the thin-layer effects acting in sand and clays. Figure 11 illustrates the expected thin-layer effects in (a) a thin clay layer in sand and (b) a thin sand layer in clay due to the difference in sensing and developing distances.

### 6.2 Layer interface detection

Based on the studied experiments, layer interfaces between sand and clay may be interpreted based on representative extreme values of  $m$ . The top interface of clay layers can be approximated at a depth with an extreme value of  $m$  less than  $-0.4$ . For layers with small contrast in characteristic cone resistance, such as the two-layered sand/ or clay, a value of about  $-0.2$  can indicate a layer interface. A bottom interface of a clay layer may be interpreted at the depth where the parameter  $m$  reaches an extreme positive value of at least  $0.5$ .

## 7 CONCLUSIONS

A cone resistance rate of change parameter shows promising possibilities to detect layer interfaces between sand and clays. The parameter additionally yields useful information on transition effects. It allows for efficient interpretation of layer boundaries and may even detect layers as thin as the cone diameter. The use of the parameter for interface detection depends on a significant contrast in characteristic cone resistance between layers. Testing on field data is needed to look deeper into the possibilities and the limitations for this method of layer interface detection in naturally formed deposits.

## REFERENCES

- Boulangier, R., & DeJong, J. 2018. Inverse filtering procedure to correct cone penetration data for thin-layer and transition effects. *Proceedings of the 4th International Symposium on Cone Penetration Testing (CPT'18)*, Delft, 21-22 June.
- de Lange, D.A. 2018. *CPT in Thinly Layered Soils* (J. van Elk & D. Doornhof, Eds.; No. 1209862-006-GEO-0007).
- Hammer, H.B. 2020. *Physical experiments on CPTU thin-layer effects of thin clay layers embedded in sand* (Master's thesis). Norwegian University of Science and Technology (NTNU), Trondheim, Norway. 11250/2689484
- Hammer, H.B., Nordal, S. and L'Heureux, J.-S. In press. Detection of thin clay layers in sand using a standard CPTU probe. *20th International Conference on Soil Mechanics and Geotechnical Engineering (ICSMGE)*, Sydney, 1-5 May.
- Hird, C., Johnson, P., & Sills, G. 2003. Performance of miniature piezocones in thinly layered soils. *Geotechnique*, 53(10),885-900. 10.1680/geot.2003.53.10.885
- Młynarek, Z., Gogolik, S., & Póltorak, J. 2012. The effect of varied stiffness of soil layers on interpretation of CPTU penetration characteristics. *Archives of civil and*

- mechanical engineering*, 12(2),253–264. 10.1016/j.acme.2012.03.013
- Teh, K. L., Leung, C. F., Chow, Y.K. & Cassidy, J. 2010. Centrifuge model study of spudcan penetration in sand overlying clay. *Géotechnique*, 60(11),825–842. 10.1680/geot.8.P.077
- Tehrani, F.S., Arshad, M. I., Prezzi, M., & Salgado, R. 2017. Physical modeling of cone penetration in layered sand. *Journal of Geotechnical and Geoenvironmental Engineering*, 144 (1).10.1061/(ASCE)GT.1943-5606.0001809
- Skrede, H. 2021 *CPTU-detection of thin clay layers in sand* (Master's thesis). Norwegian University of Science and Technology (NTNU). Trondheim, Norway.
- van den Berg, P. 1994. *Analysis of soil penetration*. (Doctoral dissertation, Delft University of Technology).
- van der Linden, T.I., De Lange, D.A., & Korff, M., 2018. Cone Penetration Testing in Thinly Inter-Layered Soils. *Geotechnical Engineering*. 10.1680/jgeen.17.00061
- Wang, Y. 2019. *Centrifuge Modelling and Numerical Analysis of Penetrometers in Uniform and Layered Clays*. (Doctoral dissertation, The University of Western Australia). 10.26182/5d14603a91815
- Youd, T.L. and Idriss, I.M. 2001. Liquefaction resistance of soils: summary report from the 1996 NCEER and 1998 NCEER/NSF workshops on evaluation of liquefaction resistance of soils. *Journal of Geotechnical and Geoenvironmental Engineering*, ASCE, 127(4),297–313. 10.1061/(ASCE)1090-0241(2001)127:4(297)